EXPERIMENTAL STUDIES OF SPANWISE CORRELATION IN AN ACTUATED TURBULENT BOUNDARY LAYER

Mitchell Lozier, Flint O. Thomas, Stanislav Gordeyev
Dept. of Aerospace and Meceqhanical Engineering
University of Notre Dame
Hessert Laboratory, Notre Dame, IN 46556, USA
sgordeye@nd.edu

ABSTRACT

In this study we introduce a two-dimensional, periodic, synthetic large-scale structure into a moderately low Reynolds number turbulent boundary layer and investigate the boundary layer response to this synthetic structure through spanwise correlations of the streamwise velocity. Two hot-wire probes, with variable spanwise offset, were placed in the near-wall and log-linear region of the boundary layer to measure these correlations. Results indicate that the magnitude of the correlation changes depending on the phase of the periodic synthetic structure. Additionally, changes in the spanwise correlation were observed in both the near-wall and log-linear regions, with the largest variations seen in the log-liner region. The maximum correlation magnitudes were found to be synchronized with the passing of the convecting synthetic structure, while the correlation magnitudes relax back to canonical levels in between. These elevated correlation magnitudes related to the synthetic large-scale structure dynamics indicate a possibility of localized and transient changes to the dynamics of the near-wall structure.

INTRODUCTION

It is widely recognized that large-scale structures (LSS) play an important role in governing the dynamics of wall-bounded turbulent flows. In turbulent boundary layers (TBL) for example, the effects of these LSS on technologically relevant flow properties (e.g friction drag, noise generation, aero-optical distortion, flow separation, etc.) have been extensively documented (Robinson, 1991; Hutchins & Marusic, 2007). The presence of LSS in the TBL is evident from the energetic and organized large-scale motions which can be observed in the log-linear region of flows with sufficiently high Reynolds number ($Re_\tau > 2000$ Robinson (1991)). These LSS are comprised of groups, or packets, of coherent vortical structures, which are often described as having a hairpin shape, and which scale with the boundary layer thickness. Interestingly, the LSS dynamics have been found to be strongly correlated with small-scale turbulence dynamics near the wall, and this correlation strengthens with Reynolds number (Hutchins & Marusic, 2007).

This near-wall turbulence also contains coherent structures, observed within the buffer region ($5 < y^+ < 30$), comprised of unsteady small-scale quasi-streamwise vortices and the streaks of low- or high-speed fluid between them. These vortices have an inherent sense of order with a typical spanwise separation of $\Delta z^+ = 100$ and streamwise wavelength of $\lambda_x^+ = 1000$, both of which are independent of the Reynolds number (Robinson, 1991; Kline et al., 1967). These vortices also create a streamwise velocity field which is highly variable and even inflectional across the spanwise direction (i.e. low- and high-speed streaks) lending to their unsteadiness (Antonia & Bisset, 1990). These unsteady near-wall vortices can then cause intermittent and quasi-cyclic events whereby low-speed fluid is ejected away from the wall and high-speed fluid is entrained towards the wall. These so-called bursting events are responsible for the elevated shear stress in the near-wall region which also accounts for the significant production of turbulence near the wall. As such, the amplitude and arrangement of these streamwise vortices and streaks, along with the dynamics of the bursting events, regulate important flow properties such as skin friction.

Although this near-wall turbulence production cycle appears to be largely self-sustaining it is believed that the natural large-scale structures in the TBL have at least a modulating effect on near-wall events. These findings suggest that flow control strategies targeting LSS dynamics in the TBL could be effective in achieving technological goals (e.g. drag reduction, noise reduction or separation control) which are directly related to near-wall dynamics as described above. Such strategies could lead to significant performance gains and cost savings in application. However, to date, this potential remains largely unrealized due, in large part, to an incomplete understanding regarding the formation, evolution and interaction of LSS within the near-wall and outer regions of the TBL. We take the view that in order to clarify the dynamics of large-scale structures, one needs to analyse the flow's response to an external perturbation. Such a dynamic systems approach in which the boundary layer is perturbed via an active control actuator is particularly well suited to gaining insights regarding the underlying flow physics which is essential for the development of novel flow control strategies. To that end, a well defined perturbation with a known frequency and/or spatial wavelength can be introduced artificially to analyse the non-linear response of the TBL. This approach then allows, for instance, the study of interactions between various coupled scales of motion and provides a well-defined phase reference by which to perform phase-locked analysis. In this manner, controlled periodic perturbations have been experimentally introduced into turbulent boundary layers previously through dynamic (temporally oscillating) wall roughness (McKeon et al., 2018) and through forced shear layers in the outer region

(Ranade *et al.*, 2019). In each case the introduction of periodic perturbations at scales of interest has proven an effective way to characterize flow dynamics.

Pursing this dynamic systems approach, an active flow control device was designed for this study to introduce synthetic, organized, large-scale motions into the outer region of the turbulent boundary layer using a plasma-based actuator. The experimental boundary layer chosen for this study has a Reynolds number which is low enough that there are no naturally occurring large-scale structures in the canonical TBL. Instead, the plasma actuator introduces a controlled, spanwise-uniform, large-scale, vortical structure, with user defined streamwise wavelength and amplitude, into the outer region of the boundary layer at a user selected wall-normal location. By studying the response of the near-wall region to this synthetic structure we will comment on how the synthetic large-scale structure, introduced into the boundary layer, effects near-wall turbulence dynamics. Specifically we propose to measure the spanwise correlation of the streamwise velocity which gives an indication of the presence and arrangement of the streamwise vortices and streaks in the near-wall region.

EXPERIMENTAL SETUP

The experiments presented in this study were performed in the low-turbulence, subsonic, in-draft wind tunnel located at the Hessert Laboratory for Aerospace Research at the University of Notre Dame. Experiments were performed in a test section of 0.6 *m* square cross-section and 1.82 *m* length. For this study, a flat, 2-meter-long, boundary layer development plate was used. The boundary layer development plate spanned the full test section width and was installed along the center height of the test section with a sandpaper distributed roughness element attached to the leading edge.

A plasma-based active flow control actuator, briefly described below, was attached to the top side of the boundary layer development plate at a fixed streamwise location of $X = 140$ *cm* downstream of the leading edge of the boundary layer development plate. A set of representative canonical turbulent boundary layer parameters, measured around the actuator location, are summarized in Table 1 for reference. Full details of the experimental setup can be found in Lozier *et al.* (2024, 2023); Lozier (2023).

The plasma-based Active Large-Scale Structure Actuator (ALSSA) was used in this study to introduce periodic, spanwise-uniform, plasma–induced forcing in the outer region of the turbulent boundary layer as shown in Figure 1(a). The plasma actuator was supported above the boundary layer development plate by thin vertical NACA0010 airfoils on both sides to minimize the blockage by the plate. The actuator plate was made of a 2-mm-thick sheet of Ultem dielectric polymer. The dimensions of the actuator plate were $W = 25$ *cm* ($W = 8\delta$, $W^+ = 5600$) wide in the spanwise direction and $L = 32$ *mm* ($L < 1\delta$, $L^+ = 640$) long in the streamwise direction. The leading edge of the actuator plate was rounded, and the last 10 *mm* of the trailing edge were linearly tapered to a half-angle of 10 degrees to eliminate the separation region downstream of the trailing edge of the actuator plate. The distance between the actuator and wall was fixed at $H = 0.3\delta$ ($H^+ = 200$). Thin copper electrodes were attached to the top and bottom side of the actuator plate in order to create a spanwise-uniform plasma jet on the top side of the actuator plate. An upper surface electrode of 0.05-mm-thick copper foil tape was located 15 *mm* from the plate leading edge and was 4 *mm* in length and 22 *cm* in width. On the lower surface, a

second copper foil electrode was located 15 *mm* from the leading edge, aligned with the top electrode, and was 12 *mm* in length and again 22 *cm* in width. The positioning of the electrodes with respect to the leading edge of the dielectric plate and the width of the electrodes were carefully selected to prevent arcing between the top and bottom electrodes around the edges of the dielectric plate. The alternating current dielectric barrier discharge (AC-DBD) plasma was produced using a high voltage (40 *kV* peak-to-peak) AC source which provided sinusoidal excitation to the actuator electrodes at a frequency of 4 *kHz*. At this frequency the plasma jet is quasisteady (Thomas *et al.*, 2009). To introduce periodic forcing, the sinusoidal excitation waveform was modulated by a square wave with a 50/50 duty cycle oscillating at the $f_P = 80$ *Hz* forcing frequency. All characteristics of the plasma actuator design and operation were optimized for our specific experimental TBL (Lozier *et al.*, 2024).

To measure spanwise correlations, a constant temperature anemometer (CTA) with two boundary layer style hot-wire probes (Dantec 55P15) with diameters of 5 *μm* and lengths of $l = 1.5$ *mm* ($l^+ = 30$) were used to collect time series of the streamwise component of velocity across a range of spanwise separations, see Figure 1(b). The sampling frequency was $f_S = 30$ *kHz* and the sampling time was $T_S = 90$ *s* for each case such that $t^+ = u_\tau^2/(f_S\nu) \approx 0.2$ and $T_S U_\infty/\delta_{99} \approx 19000$. The first hot-wire was held stationary at the mid span of the test section. The second hot-wire, mounted on a spanwise oriented traversing stage, was attached to the stationary hot-wire and matched in x- and y-position. Measurements were taken simultaneously with the hot-wires starting at a minimum separation of $\Delta z = 2$ *mm* ($\Delta z^+ = 40$) and reaching a maximum separation around $\Delta z = 1.1\delta$.

For all of the results presented here the probes were positioned at the furthest downstream location achievable, $x = 8\delta$, as measured downstream of the plasma actuator's trailing edge. The results presented here will focus on the wall-normal positions of $y^+ = 25$ and $y^+ = 100$ which correspond to the near-wall and log-linear regions of the TBL.

RESULTS

In previous measurements, it was demonstrated that the synthetic large-scale motions induced by the plasma actuator modulate small-scale turbulence amplitudes in the near-wall region (Lozier *et al.*, 2024). The actuator was also designed to be spanwise-uniform over a large extent such that three-dimensional end effects of the actuator plate will not influence measurements (Lozier *et al.*, 2024). Now, in order to further investigate what effect the synthetic LSS has on the organization and dynamics of the near-wall cycle, velocity correlations will be computed using the two spanwise offset hot-wires. To quantify the spanwise correlation of the streamwise velocity between the two hot-wire probes, a standard two-point normalized correlation coefficient, R_z, presented in Equation 1 was computed.

$$R_z(x,y,\Delta z) = \frac{\overline{u(x,y,z,t)u(x,y,z+\Delta z,t)}}{\sqrt{\overline{u(x,y,z,t)^2}}\sqrt{\overline{u(x,y,z+\Delta z,t)^2}}} \quad (1)$$

An example spanwise correlation coefficient profile for the canonical TBL (no actuator) is shown in Figure 2(a). In the log-linear region ($y^+ = 100$) the first crossing from positive to negative correlation is around $\Delta z = 0.25$ ($\Delta z^+ = 170$)

δ_{99}	δ^*	θ	U_∞	u_τ	c_f	H_S	Re_θ	Re_τ
$33\ mm$	$5.1\ mm$	$3.8\ mm$	$7\ m/s$	$0.31\ m/s$	0.0039	1.36	1760	690

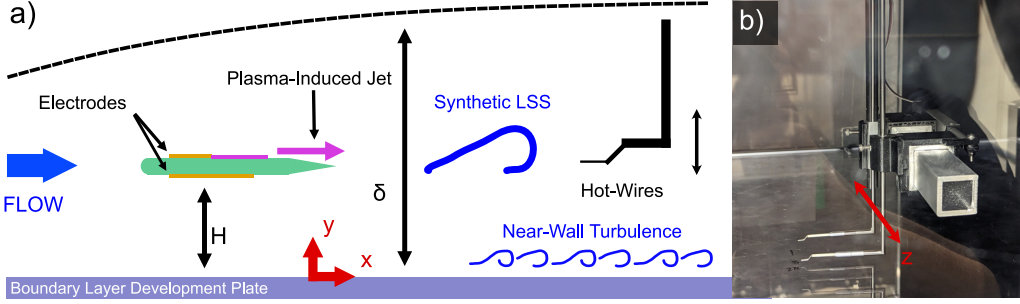Table 1.   Turbulent boundary layer parameters at the measurement location.

Figure 1.   (a) Schematic of experimental setup. (b) Photograph of spanwise traversing hot-wire stage.

which is consistent with the typical spanwise scale of δ-scaled vortical structures (Ganapathisubramani *et al.*, 2005). The data is plotted along with published results for a canonical boundary layer with similarly low Re_τ at a similar wall-normal location (Ganapathisubramani *et al.*, 2005) and good agreement between the profiles is observed. The spanwise correlation coefficient profiles for our experimental canonical TBL across a range of wall-normal locations are shown in Figure 2(b). Looking at the first zero-crossing of each profile, there is a clear growth in spanwise coherence which is dependent on wall-normal location, from $y^+ = 25$ up to $y^+ = 350$ ($y/\delta = 0.5$). This behavior is both expected and consistent with previous studies (Tomkins & Adrian, 2003). Closer to the wall the zero-crossing is approaching the reported value of $\Delta z^+ = 100$ ($\Delta z/\delta = 0.15$) which corresponds to the typical near-wall structure (Antonia & Bisset, 1990). However, the measurements here are limited towards the upper limit of the buffer region, and as such we do not reach the expected value exactly, although it is being approached. The agreement observed in the characteristics of the canonical spanwise correlation profiles shown here validate our method.

Spanwise correlations for the canonical (no actuator), plate only (no active plasma forcing), and plasma on cases in the near-wall and log-linear regions are compared in Figure 3. At each wall-normal location the addition of the actuator plate alone does not result in a modification of the spanwise correlation as compared to the canonical case. However, there is a positive shift in the spanwise correlation, at the largest separation distances, when the plasma forcing is active. In both locations, but specifically in the log-linear region, the first zero crossing of the profile does not change location indicating that there is no net effect of the plate or plasma forcing on the spanwise coherence of vortical structures.

However, this correlation is an average measure, and in the case of active plasma forcing it is useful to decompose the velocity time series which has been phase-locked to the plasma forcing. We start with a decomposition of the instantaneous velocity time series $\hat{u}(y,z,t) = U(y) + u(y,z,\phi,n)$. Here $U(y)$ is the local mean streamwise velocity and $u(y,z,\phi,n)$ is a phase dependent streamwise velocity fluctuation. The velocity time series are split into blocks with a duration of one actuation period, $T_P = 1/f_P$, where the phase of the actuation period is $\phi = 2\pi(t_n/T_P - n)$, and n is the block number. The phase dependent fluctuations $u(y,z,\phi,n)$ can be ensemble averaged over n blocks to compute a modal velocity, $\tilde{u}(y,z,\phi)$, which is phase-

locked to the plasma forcing. An ensemble root-mean-square of residual fluctuations, $u'(y,z,\phi,n) = u(y,z,\phi,n) - \tilde{u}(y,z,\phi)$, can also be computed to quantify the phase dependent behaviour of smaller-scale fluctuations. Phase averaged changes in this quantity, $\Delta u'_{RMS}$, will be referred to as the residual turbulence, and will be used to represent an envelope of the small-scale fluctuation amplitudes which are coupled to the plasma forcing (Lozier *et al.*, 2024). Using this phase-locked decomposition, a phase dependent two-point correlation coefficient was also computed by averaging over the number of blocks, as demonstrated in Equation 2,

$$R_{z,\phi}(y,\Delta z,\phi) = \frac{\langle u(y,z,\phi,n)u(y,z+\Delta z,\phi,n)\rangle_n}{\sqrt{\langle u(y,z,\phi,n)\rangle_n^2}\sqrt{\langle u(y,z\Delta z,\phi,n)\rangle_n^2}} \quad (2)$$

As a final step, similar to the residual turbulence quantity, the phase average of the phase dependent correlation was removed in order to analyze phase dependent changes in the spanwise correlation, later labelled as $\Delta R_{z,\phi}$ (Figure 5).

First, the spanwise variation of the modal velocity and residual turbulence are shown in Figure 4. These plots demonstrate that, as shown in previous studies Lozier *et al.* (2023, 2024), the plasma forcing induces strong large-scale motions in the regions below the actuator, Figure 4(a,c). The plasma forcing also modulates the amplitude of small-scale turbulent fluctuations as seen in Figure 4(b,d). The overlap of the profiles in Figure 4 across all spanwise separations shows that the synthetic LSS is also sufficiently spanwise-uniform for this study. Detailed analysis and discussion of the organizing and modulating effects of the synthetic LSS on the turbulent boundary layer can be found in Lozier *et al.* (2023, 2024).

Phase-locked measurements of the spanwise correlation for a single separation distance are shown in Figure 5. The average spanwise correlations are shown as horizontal red lines which correspond to the encircled points in Figure 3. The peaks in the phase dependent spanwise correlation ($R_{z,\phi,MAX}$), and minimums ($R_{z,\phi,MIN}$), were identified at each spanwise separation, as shown in Figure 5(a). From previous studies, it is known that the the streamwise position of the synthetic LSS is positively correlated with, and leading, the peaks in residual turbulence below the actuator. This suggests that the maximum correlation occurs just upstream of, i.e. a small phase lag with respect to, the synthetic LSS passing in the outer region. Closer to the wall, the correlation magnitude is also smaller
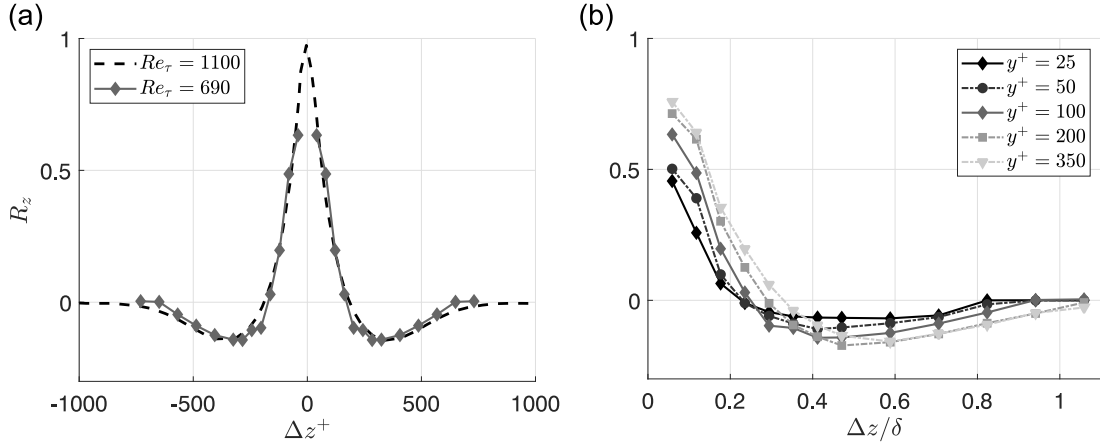
Figure 2. Spanwise profiles of the streamwise velocity correlation for the canonical TBL at (a) $y^+ = 100$ overlaid with low Reynolds number data ($Re_\tau = 1100$, $y^+ = 92$) from Ganapathisubramani *et al.* (2005) and (b) all wall-normal locations with lighter colors indicating larger distance from the wall. Locations of interest shown with diamond markers and solid lines. $x = 8\delta$
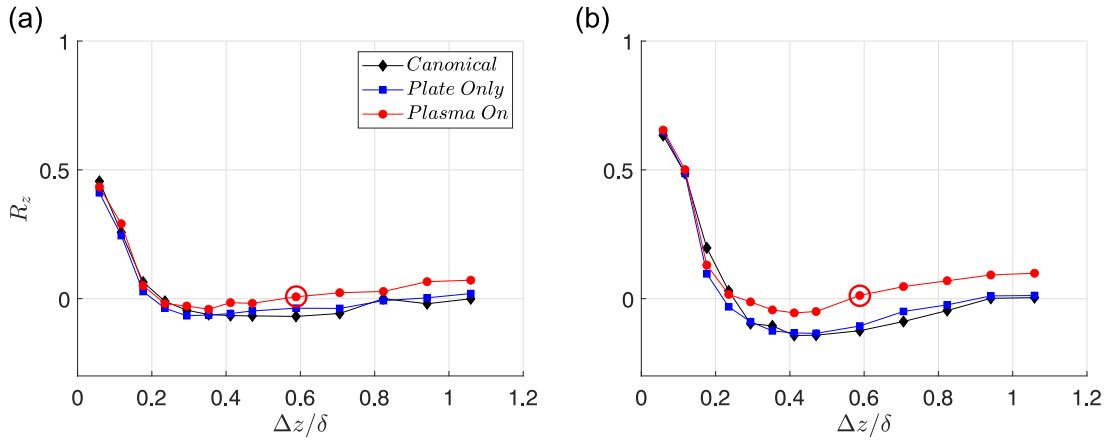

Figure 3. Spanwise profiles of streamwise velocity correlation for canonical, plate only, and plasma on cases at (a) $y^+ = 25$ and (b) $y^+ = 100$. Red circled points correspond to horizontal red lines in Figure 5. $H^+ = 200$, $x = 8\delta$, $f_P = 80\,Hz$

than it is in the log-linear region which is expected as the later is physically closer to the synthetic LSS.

Fluctuations about the average spanwise correlation ($\Delta R_{z,\phi}$) were also computed as shown in Figure 5(b). By computing this quantity across all separation distances a map of the phase dependent fluctuations in the spanwise correlation can be created as shown in Figure 6. From this map it is clear that these fluctuations are uniform in the spanwise direction and extend from the smallest separation distance to over δ. The largest variations in the spanwise correlation were observed at a wall-normal location of $y^+ = 200$ (not shown), which is in line with the actuator height. At this wall-normal location the phase of peak positive correlation occurs at approximately $\phi = \pi/2$ across all separation distances. Moving closer to the wall, the peak in positive correlation moves to later phases reaching $\phi = \pi$ both inside the log-region ($y^+ = 100$), see Figure 6(a), and near the wall ($y^+ = 25$), Figure 6(b). Across all wall-normal locations the peak in positive correlation appears independent of separation distance. Therefore the conclusions from Figure 5 can be applied across all separation distances. This provides a full picture of how the spanwise correlation is varying with phase, spanwise separation and wall-normal distance.

The maximum and minimum amplitude of the spanwise correlation can be used to isolate effects relative to the passing of the synthetic LSS. These results are shown in Figure 7 for

the streamwise location of $x = 8\delta$ downstream of the actuator. Now we can see that sufficiently far downstream there still is a strong effect on the spanwise correlation, demonstrated by the red dotted lines in Figure 7 as the synthetic LSS is passing above this streamwise location. However, between passing of the synthetic LSS, the correlation magnitudes relax back to canonical (or plate only) levels as shown by the dashed blue lines. When the spanwise correlation was measured near the wall, $y^+ = 25$, see Figure 7(a), there was not a strong effect on the spanwise correlation in the presence of the LSS, compared to the location of $y^+ = 100$ away from the wall, see Figure 7(b). This indicates that the synthetic LSS only has a local organizing effect. This local deviation in the correlation, over large spanwise separations, from the canonical values suggests that the spanwise-uniform, synthetic, large-scale motions induced by the actuator become the dominant flow features as the synthetic LSS convects past a specific streamwise location. But this is highly transient as the canonical TBL structure can be seen in the spanwise correlation profile in between each passing. Overall these results indicate there is no lasting modification of the near-wall TBL structure by the synthetic LSS. However, locally there may be changes to the near-wall dynamics as the induced large-scale motions become a dominant feature of the flow in the near-wall region.

These preliminary results show evidence of the transient regulating effect the synthetic LSS has throughout the
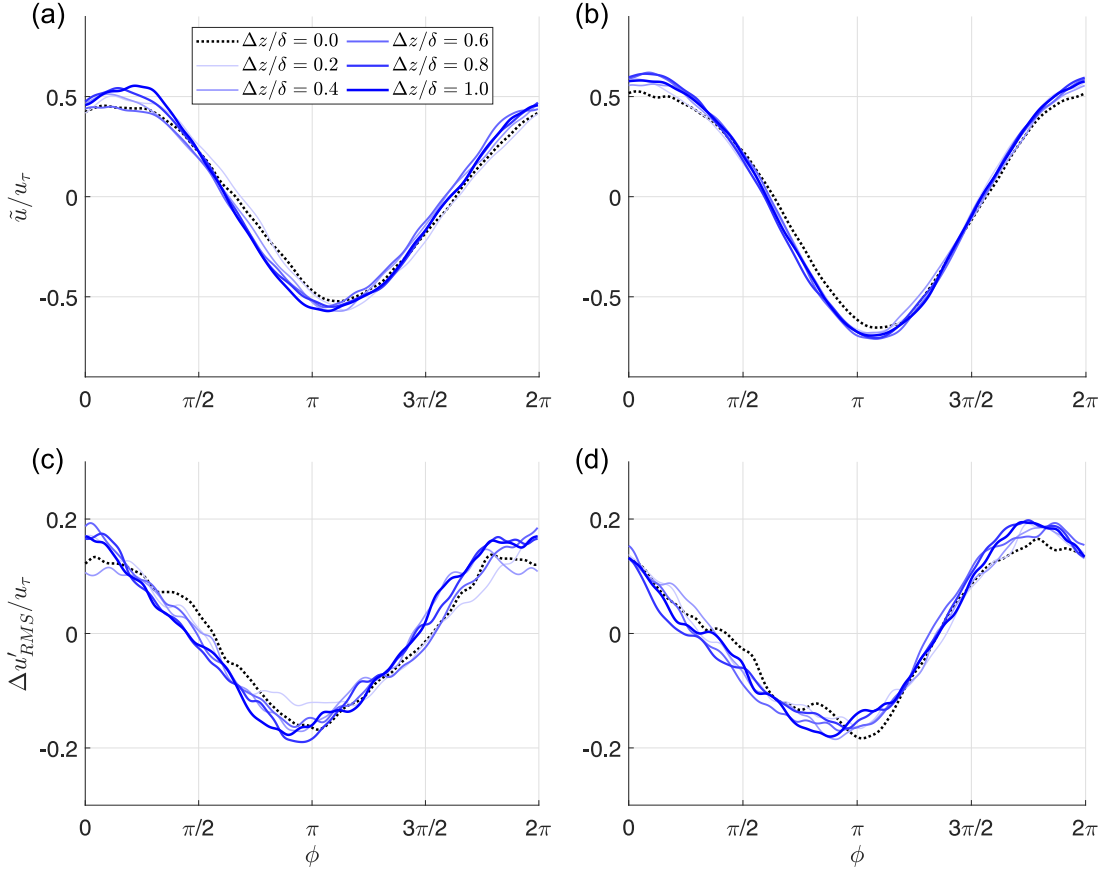
Figure 4. Phase dependent variations in (a,b) modal velocity and (c,d) residual turbulence at (a,c) $y^+ = 25$ and (b,d) $y^+ = 100$ across multiple spanwise locations. $H^+ = 200$, $x = 8\delta$, $f_P = 80\,Hz$
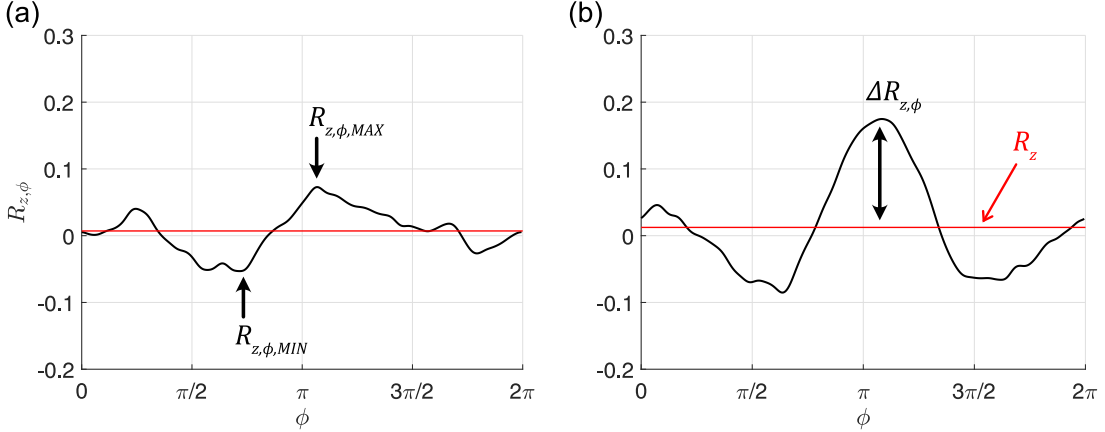

Figure 5. Phase dependent variation in spanwise correlation with $\Delta z = 0.6\delta$ for plasma on case at (a) $y^+ = 25$ and (b) $y^+ = 100$. Horizontal red lines correspond to circled points in Figure 3. $H^+ = 200$, $x = 8\delta$, $f_P = 80\,Hz$

boundary layer as fluctuations in streamwise velocity become strongly correlated over a large span in the presence of the synthetic LSS. This effect could have implications in modifying the dynamics of the autonomous near-wall cycle or modulating the self sustaining mechanisms of turbulence production. But, the localized nature of this modification, and the relaxation back to canonical behavior between the passing of the synthetic LSS, suggests the near-wall cycle primarily remains autonomous. Further studies using techniques like event based averaging will give a more complete picture of the effect of the synthetic LSS on near-wall dynamics and the localized effect on properties such as turbulence production and skin friction.

REFERENCES

Antonia, R. A. & Bisset, D. K. 1990 Spanwise structure in the near-wall region of a turbulent boundary layer. *Journal of Fluid Mechanics* **210**, 437–458.

Ganapathisubramani, B., Hutchins, N., Hambleton, W. T., Longmire, E. K. & Marusic, I. 2005 Investigation of large-scale coherence in a turbulent boundary layer using two-point correlations. *Journal of Fluid Mechanics* **524**, 57–80.

Hutchins, N. & Marusic, I. 2007 Large-scale influences in near-wall turbulence. *Philosophical Transactions of the Royal Society A: Mathematical, Physical and Engineering Sciences* **365** (1852), 647–664.
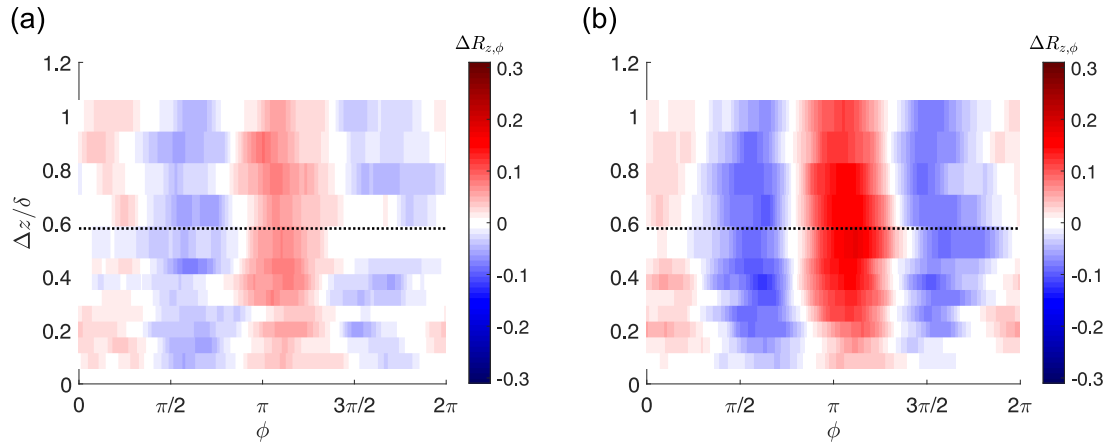
Figure 6. Phase dependent variation of spanwise correlation for plasma on case across all spanwise separation distances at (a) $y^+ = 25$ and (b) $y^+ = 100$. Dotted lines correspond to profiles in Figure 5. $H^+ = 200$, $x = 8\delta$, $f_P = 80\ Hz$
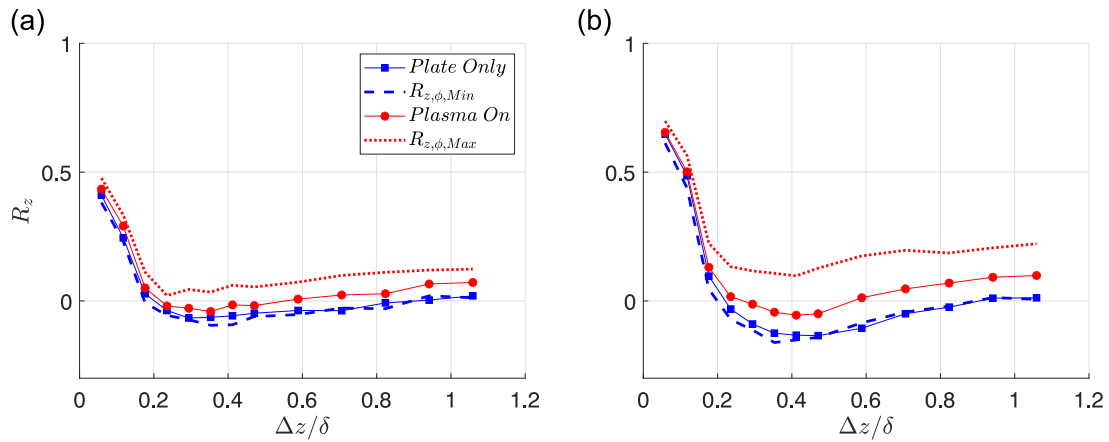

Figure 7. Spanwise profiles of streamwise velocity correlation for plate only and plasma on cases at (a) $y^+ = 25$ and (b) $y^+ = 100$. Maximum and minimum phase dependent correlation shown as dashed and dotted lines respectively. $H^+ = 200$, $x = 8\delta$, $f_P = 80\ Hz$

Kline, S. J., Reynolds, W. C., Schraub, F. A. & Runstadler, P. W. 1967 The structure of turbulent boundary layers. *Journal of Fluid Mechanics* **30** (4), 741–773.

Lozier, M. 2023 Characterization of Turbulent Boundary Layer Dynamics via Active Manipulation of Large-Scale Structures. PhD thesis, University Of Notre Dame.

Lozier, M., Thomas, F. O. & Gordeyev, S. 2023 Experimental investigation of turbulent boundary layer dynamics via active manipulation of large-scale structures. *International Journal of Heat and Fluid Flow* **103**, 109194.

Lozier, M., Thomas, F. O. & Gordeyev, S. 2024 Response of a Turbulent Boundary Layer to an Imposed Synthetic Large-Scale Structure. *AIAA Journal* **62** (2), 573–589.

McKeon, B. J., Jacobi, I. & Duvvuri, S. 2018 Dynamic Roughness for Manipulation and Control of Turbulent Boundary Layers: An Overview. *AIAA Journal* **56** (6), 2178–2193.

Ranade, P., Duvvuri, S., McKeon, B. J., Gordeyev, S., Christensen, K. & Jumper, E. J. 2019 Turbulence Amplitude Amplification in an Externally Forced, Subsonic Turbulent Boundary Layer. *AIAA Journal* **57** (9), 3838–3850.

Robinson, S. K. 1991 Coherent Motions in the Turbulent Boundary Layer. *Annual Review of Fluid Mechanics* **23**, 601–639.

Thomas, F. O., Corke, T. C., Iqbal, M., Kozlov, A. & Schatzman, D. 2009 Optimization of Dielectric Barrier Discharge Plasma Actuators for Active Aerodynamic Flow Control. *AIAA Journal* **47** (9), 2169–2178.

Tomkins, C. D. & Adrian, R. J. 2003 Spanwise structure and scale growth in turbulent boundary layers. *Journal of Fluid Mechanics* **490**, 37–74.